Eur. Phys. J. B **49**, 213–218 (2006)
DOI: 10.1140/epjb/e2006-00053-9

THE EUROPEAN PHYSICAL JOURNAL B

Quantum Hall bilayer digital amplifier

R. Khomeriki[1], J. Léon[2,a], and D. Chevriaux[2]

[1] Physics Department, Tbilisi State University, 0128 Tbilisi, Georgia
and
Dipartimento di Energetica "S. Stecco", Università di Firenze, 50139 Firenze, Italy
[2] Laboratoire de Physique Théorique et Astroparticules, CNRS-UMR5207, Université Montpellier 2, 34095 Montpellier, France

Received 10 November 2005
Published online 17 February 2006 –

Abstract. A quantum Hall double layer system at total Landau level filling factor $\nu = 1$, seeded by a modulated ac-voltage input signal of frequency inside the forbidden band gap, is demonstrated to work as a digital amplifier of ultra weak signals. The theory employs to the sine-Gordon model and it is confirmed by the first experimental observations of nonlinear bistable transmission in a pendula chain.

PACS. 73.43.Lp Collective excitations – 05.45.-a Nonlinear dynamics and nonlinear dynamical systems – 05.45.Yv Solitons

1 Introduction

When a system submitted to a given external excitation manifests two different and persistent responses, it is said to be bistable. Bistability is a fundamental property at the origin of hysteresis, as revealed originally in magnetic materials. Recent works have shown that nonlinearity in a wave equation can intrinsically lead to bistable transmission when the medium is submitted to boundary driving or wave scattering. More precisely, when the excitation is a periodic signal of frequency in a forbidden band-gap, that normally has a vanishing transmission coefficient, the system may switch to a high transmission state by the mediation of nonlinear excitations.

This *nonlinear bistable transmission* (NBT) has been investigated both theoretically and experimentally in nonlinear optical materials [1–5] and numerically in Josephson junctions [6–8]. Although such systems are of different physical nature, NBT has a common origin, the *nonlinear supratransmission* property [9–13]. Then the NBT process has been given a comprehensive analytical approach by means of the exact stationary solutions of the sine-Gordon and nonlinear Schrödinger equations on the finite interval submitted to a periodic boundary forcing [14,15].

The importance of predicting NBT in a nonlinear medium is its application to elaborate particular devices as switches, logic gates, memories, ultra-sensitive detectors or amplifiers. Moreover its universality allows to conceive such devices in a vast variety of nonlinear systems possessing a forbidden band-gap : spin chains, Bose-Einstein condensates, magnetic thin films, Josephson junctions transmission lines or fiber guide arrays.

We consider here a quantum Hall double layer system [16] at Landau level filling factor $\nu = 1$, which possess properties similar to superconducting Josephson junctions [17–21]. By submitting the system to a boundary ac-voltage driving, we predict the existence of bistable behaviour, demonstrate that the system may respond to ultra weak applied signals and, under convenient modulation of the seed boundary driving, discover through numerical simulations that it can work as a digital amplifier. By *digital amplifier* we understand a device acting as a transducer of a sequence of low amplitude step-like signals to the same sequence with significantly large amplitude output. In the numerical simulations made to sustain our proposal, we obtain for an input signal of amplitude 0.15 μV and duration 100 ns, an output signal of amplitude 30 μV and duration 110 ns.

The theory is then sustained and illustrated by the first experimental observation of NBT in a pendula chain, which shares with the quantum Hall bilayer the property to obey the sine-Gordon model. Despite the intrinsic rough quality of a mechanical chain, we obtain remarkable agreement with the analytical description. The experimental setup appears then as a simple, still spectacular, didactic tool to demonstrate nonlinear bistable transmission.

2 The driven quantum Hall bilayer

2.1 The model

A quantum Hall bilayer system [16–21] consists of electrons confined in closely separated two dimensional semiconductor layers submitted to intense magnetic field. In

[a] e-mail: jleon@lpta.univ-montp2.fr

the absence of interlayer voltage, each layer of the system has a filling factor $\nu = 1/2$. Because the layers are identical, an electron in one layer can be identified with a pseudo-spin up, and in the other layer with a pseudo-spin down. It is clear that the system has the lowest energy when all pseudo-spin lie in the plane, reflecting the fact that in the ground state the electrons are equally distributed between the two layers.

Within such a formalism, a double layer quantum Hall system is treated as an easy plane ferromagnet with a hard axis anisotropy. An electron tunneling between the layers corresponds there to a spin flip. Consequently, just like ordinary easy axis ferromagnetic systems [22,23], the low energy dynamics of the quantum Hall bilayer submitted at one end to an ac interlayer voltage V is described by the boundary-driven and damped sine-Gordon equation with a free end [21]

$$\frac{\partial^2 u}{\partial t^2} - 8\beta\rho(2\pi\ell^2)\frac{\partial^2 u}{\partial x^2} + 8\beta\Delta\,\sin u + \gamma\frac{\partial u}{\partial t} = 0, \qquad (1)$$

$$\left.\frac{\partial u}{\partial t}\right|_{x=0} = \frac{e}{\hbar}V_{in}(t)\ , \quad \left.\frac{\partial u}{\partial x}\right|_{x=d} = 0. \qquad (2)$$

The field $u(x,t)$ stands for the pseudo-spin in-plane (dimensionless) phase variable and the voltage across the barrier at distance x is given by

$$V(x,t) = \frac{\hbar}{e}\,\frac{\partial u(x,t)}{\partial t}. \qquad (3)$$

The parameter β gives the hard axis anisotropy, it is related to the bilayer capacitance. Δ is a tunneling amplitude, ℓ is a magnetic length, ρ an in-plane pseudo-spin stiffness and γ is a phenomenological damping constant (dissipation). The the bilayer extends on $x \in [0,d]$. For future use as an example, we list the values of these parameters as found in [24,25] (units $\hbar = e = k_B = 1$ for which frequencies read in Kelvin by the relation $1\,\mathrm{K} = 1.38 \times 10^{11}\,\mathrm{s}^{-1}$):

$$\ell = 40\,\mathrm{nm},\ \beta = 7\,\mathrm{K},\ \Delta = 8\times 10^{-5}\,\mathrm{K},\ \rho = 0.1\,\mathrm{K}, \qquad (4)$$

for which the band gap edge (see below) is $\omega_0 \sim 10\,\mathrm{GHz}$.

As a matter of fact, the linear dispersion relation of the model (1) shows the existence of a forbidden band gap. Consequently, a bilayer with all electrons initially equally distributed, will not respond, in the linear regime, to a boundary interlayer voltage $V_{in}(t)$ with its frequency inside the band gap, namely with

$$V_{in}(t) = V_0\ \sin(\omega t), \quad \omega^2 < \omega_0^2 = 8\beta\Delta. \qquad (5)$$

In the nonlinear regime however the system will acquire stationary solutions expressed in terms of Jacobi elliptic functions, which, for the same boundary driving, can well have two (or more) different expressions.

2.2 Ultra-weak signal detection

Indeed, as demonstrated in [14], and reproduced in the appendix, the sine-Gordon equation submitted to the boundary driving (5) locks to a set of 3 stationary solutions with two stable branches. Although these are neither exact solutions of the damped case, nor match *analyticaly* the boundary driving, the agreement shown by numerical simulations is quite remarkable.

The main resulting property is the existence of a threshold amplitude V_s (called *supratransmission* threshold after [9]) beyond which the system jumps from a state of vanishing output values, to a state of large output values, as a result of an intrinsic instability [10]. This threshold can be assigned as the solution of an implicit equation for given length d and frequency ω. For sufficiently large lengths, it possesses an explicit approximate value

$$V_s \sim 4\frac{\hbar\omega}{e}\arctan\sqrt{\frac{\omega_0^2}{\omega^2} - 1} \qquad (6)$$

very useful for practical applications. In the case of parameter values (4), we obtain a threshold of about $13\,\mu V$.

Then the principle of a detector is the following: when the system is driven right below the supratransmission threshold V_s by a permanent excitation (called driving seed), any superimposed signal can make it bifurcate to the excited state (large output). The amplitude of the signal that activates the bifurcation can be made as small as one wants by tuning the driving seed amplitude closer and closer to the threshold, hence realizing the *ultra-weak signal detector*. Moreover it appears from expression (6) that the very amplitude V_s of the threshold can also be tuned to low values by choosing the frequency close to ω_0 (eigenfrequency), value for which V_s vanishes.

We show now that the property can be used to conceive, under convenient choice of the driving seed, a device that would work as an ultra-sensitive digital amplifier.

2.3 Digital amplifier

The numerical simulations have revealed the existence of another threshold, say V_e, below which the system bifurcates back from a state of large output to a state of almost vanishing output. This is a phenomenological *extinction* threshold, directly related to the presence of damping, as indeed V_e vanishes when $\gamma \to 0$.

The presence of the extinction threshold allows now to conceive an amplifier that would respond to signals of weak amplitude and minimum duration. This is done by a convenient *modulation* of the periodic seed amplitude as

$$V_{in}(t) = [V_0(t) + S(t)]\ \sin(\omega t), \qquad (7)$$

$$V_0(t) = \frac{1}{2}(A_1 + A_2)\cos(\lambda t) + \frac{1}{2}(A_1 - A_2), \qquad (8)$$

$$A_1 < V_s, \quad A_2 < V_e, \quad A_1 - A_2 \sim V_s - V_e. \qquad (9)$$

Hereabove $V_0(t)$ is the seed modulation and $S(t)$ the signal to be detected assumed as a sequence of low amplitude step functions of duration greater than one period $2\pi/\lambda$ of the seed modulation. We shall use for instance

$$S(t) = A_s\ [\theta(t - t_1) - \theta(t - t_2)]\,, \qquad (10)$$

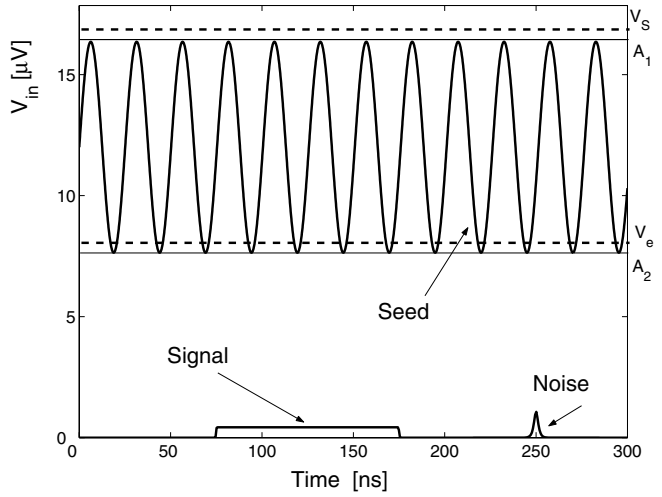

Fig. 1. Plot of the modulation amplitude $V_0(t)$ (Seed) and signal $S(t)$ (Signal+Noise) used for the input voltage (7). The included short-time pulse represents noise. The amplitudes values (straight full lines) are $A_1 = 16.3\ \mu$V, $A_2 = 7.7\ \mu$V and $A_s = 0.15\ \mu$V, the modulation frequency is $\lambda = 0.25$ GHz while the seed carrier frequency (not represented) is $\omega = \omega_0/2 = 5$ GHz. The two dashed lines show the values of the threshold voltages V_s (supratransmission) and V_e (extinction).

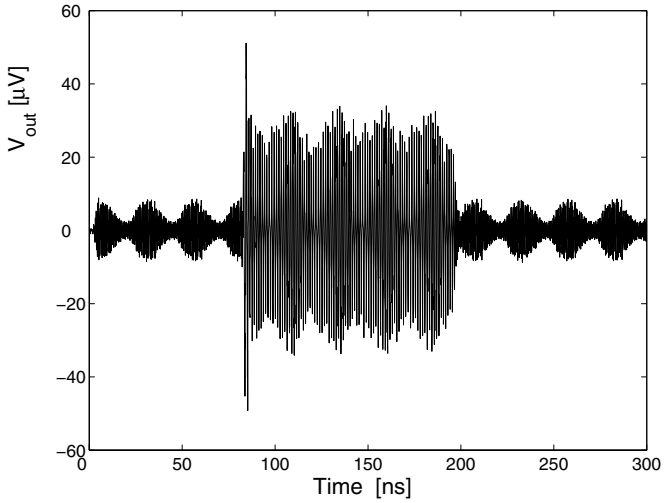

Fig. 2. Output value $V_{out}(t)$ obtained by numerical integration of (1) submitted to the boundary driving of Figure 1 with a sample length $d = 30\,\mu$m (normalized length $L = 3.9$) and phenomenological damping $\gamma = 0.1\,\omega_0$.

as representative of a square signal of amplitude A_s and duration $t_2 - t_1$ (θ stands for the Heaviside step function).

The working principle is then quite simple: before the occurence of the signal $S(t)$, namely for $t < t_1$, the system lives in a low output state. During the application of $S(t)$, the effective applied voltage $V_{in}(t)$ overcomes the threshold V_s and the system then jumps to an excited state with large output, read as the amplified signal. As soon as $S(t)$ vanishes again, the effective applied voltage $V_{in}(t)$ decreases below the extinction threshold V_e and the system bifurcates back to an almost vanishing output state.

This is demonstrated by a numerical simulation where the input voltage is represented in Figure 1 with parameters defined in the caption. The result of the simulation is summarized in Figure 2 which represents the plot of the output voltage $V_{out}(t)$ obtained by integration of (1) under boundary input (7) with parameters defined in Figure 1. The input signal results to be amplified by a factor 200 while the short duration noise does not produce a response (its duration is less than a modulation period).

3 The pendula chain

The pendula chain and the quantum Hall bilayer have in common to obey the same model, the sine-Gordon equation. The purpose of this section is to demonstrate experimentally the bistability of the periodically driven pendula chain and to compare measures with theory.

The experimental device is the linearly coupled pendula chain presented in Figure 3 and built following [26,27]: each pendulum rotate freely around a fixed guide (piano wire stretched between two supports) and is

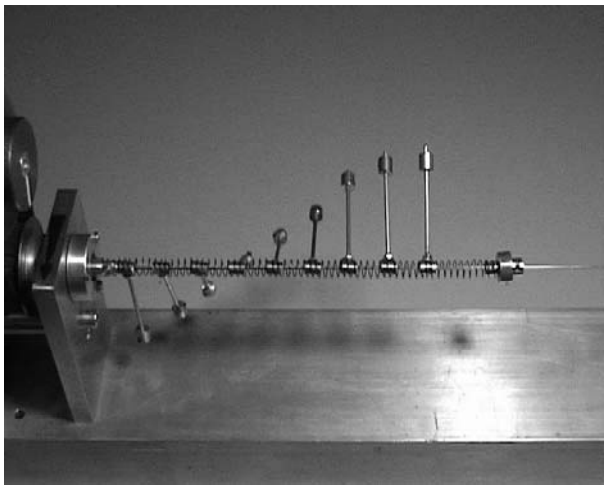

Fig. 3. The pendula chain used for the experiments. pictured in the excited working regime where the input (periodic engine torque) has an amplitude of about 0.4 rad while the output amplitude is 2.5 rad. The angular frequency of the driving is here $0.9 \times \omega_0$ where $\omega_0 = 15.1$ Hz is the eigenfrequency of a single pendulum.

coupled to its neighbors by a coil spring acting as a linear torque. An electrical engine steered by a generator of sinusoidal tension is rigidly connected to the pendulum $n = 0$.

The dynamics of this chain is naturally described by the Frenkel-Kontorova model [28]

$$\ddot{u}_n + \delta\dot{u}_n - \sigma^2\ (u_{n+1} + u_{n-1} - 2u_n) + \omega_0^2\ \sin u_n = 0, \quad (11)$$

where overdot means derivation with respect to time. The variable u_n is the angular deviation of the n$^t h$ pendulum, ω_0 is the eigenfrequency of a single pendulum and σ is proportional to the linear torsion constant of the spring.

The damping coefficient δ is phenomenological. The applied periodic driving is here modelized by the boundary value

$$u_0(t) = b\ \cos(\omega t), \tag{12}$$

while the free end leads to

$$u_{N+1}(t) = u_N(t). \tag{13}$$

Low amplitude oscillations $\exp[i(kn - \omega t)]$ are characterized by the dispersion relation

$$\omega^2 = \omega_0^2 + 2\sigma^2(1 - \cos k), \tag{14}$$

which defines a phonon band gap structure. Actually such an expression allows to calculate the parameters ω_0 and σ by driving the chain at low amplitude for a given frequency inside the phonon band and measuring the resulting wave number (i.e. counting the number of pendula within a wavelength). We have obtained

$$\omega_0 = 15.1\,\text{Hz}, \quad \sigma = 32.4\,\text{Hz}. \tag{15}$$

The experiment consists then in driving the short chain of Figure 3 with a frequency in the forbidden band gap , and with an amplitude b that is varied from 0 to the threshold b_s defined in the appendix. Without external perturbation the system locks to a periodic solution with low output amplitude $u_N(t)$ which analytic continuous limit is the solution 3 of (25). By applying then an external kick [29] to the chain one makes the system bifurcate to a state of large output amplitude (as shown on the picture of Fig. 3) which analytical continuous limit expression is the solution 1 of (25).

At given driving frequency $\omega = 0.5\,\omega_0$ we have varied the driving amplitude and measured the corresponding two allowed output amplitudes by following the above procedure. The results are then reported on the graph of the analytic bistability curves in Figure 4. Despite the rather rough chain construction, the agreement is striking and the experiment appears also as a quite spectacular demonstration of the concept of *nonlinear bistable transmission*.

The analytical description detailed in the appendix allows to make prediction of behavior for various lengths (or number N of pendula). The inset of Figure 4 represents the analytical input-output angular amplitudes plots for different system lengths. In the case of very short chains ($N < 4$) a bistable regime ceases to exist, similarly with what happens in nonlinear optical media [2,5]. For long chains the analytical calculations show that to a single input amplitude there may correspond multiple (more than 3) output amplitudes. However in long chain experiments ($N > 10$) multistable regimes cannot be reached. The point is that the chain is long enough to allow for *localization* (generation of sine-Gordon breathers). The local excitations then start to move, are reflected from the free end, and prevent occurrence of stationary regimes. In the case of our experimental setup the bistable stationary states exist in the range $3 < N < 11$ (the upper limit can be slightly moved up by using driving frequencies closer to the band edge).

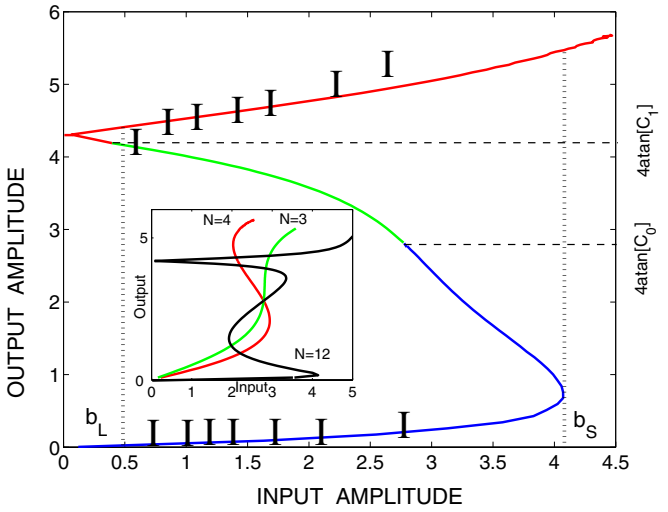

Fig. 4. Plot of the input to output angular amplitude dependence of the solution for $L = 4$ and $\Omega = 0.5$ (hence $\omega = \omega_0/2$). The graph above amplitude $4\arctan[C_1]$ corresponds to the solution (1) of (25), between $4\arctan[C_1]$ and $4\arctan[C_0]$ to the solution (2) and below $4\arctan[C_0]$ to the solution (3). The bars are the results of measurements with the driven short pendula chain. The inset presents the analytic dependence for different lengths (or pendula number) as indicated.

4 Conclusion

The analytical description of bistable stationary regimes for the sine-Gordon model, and in particular the determination of the supratransmission threshold, allowed us to propose the quantum Hall bilayer as a digital amplifier with a tunable sensitivity. The underlying working mechanism is the intrinsic bistability of the transmission property of the nonlinear medium submitted to an external excitation with a frequency belonging to the natural forbidden band gap.

Such a NBT property has been experimentally checked on a mechanical system of coupled pendula and the agreement with theory is spectacular, despite the inherent imperfections of the dispositive. This constitutes a strong indication that the process is quite generic and, most likely will manifest itself in very different physical situations.

As a matter of fact, another interesting application of the principle developed here is the Josephson junction transmission line (or the single long Jonsephson junction) which obeys also the sine-Gordon model. In that case a problem is to determine the convenient means to drive the line (or the junction). One possibility is the use of external microwave irradiation [30,31] which maps to a Neuman (instead of Dirichlet) boundary value problem for the sine-Gordon equation. Still the method can be applied and it is expected to provide interesting results [32].

R. Kh. is supported by Marie-Curie international incoming fellowship award (contract No MIF1-CT-2005-021328) and NATO grant No FEL.RIG.980767.

Appendix A: Stationary solutions

Let us first map (1) to dimensionless variables by the transformation

$$x' = x\sqrt{\Delta/(2\pi\ell^2\rho)}, \quad t' = t\sqrt{8\beta\Delta}, \tag{16}$$

and then forget the primes for convenience. The system becomes the sine-Gordon equation

$$\frac{\partial^2 u}{\partial t^2} - \frac{\partial^2 u}{\partial x^2} + \sin u + \Gamma\frac{\partial u}{\partial t} = 0, \tag{17}$$

associated with the boundary-value problem

$$u(0,t) = b\ \cos(\Omega t), \quad u_x(L,t) = 0, \tag{18}$$

for the dimensionless driving frequency (inside the band gap)

$$\Omega = \frac{\omega}{\sqrt{8\beta\Delta}} < 1, \tag{19}$$

and with the following definitions of the constants

$$b = -\frac{V_0}{\omega_0\Omega}, \quad L = d\sqrt{\Delta/(2\pi\ell^2\rho)}, \quad \Gamma = \frac{\gamma}{\omega_0}. \tag{20}$$

The stationary solutions of (17) with $\Gamma = 0$, on the finite interval $[0, L]$ submitted to the boundary conditions (18) have been derived in [14]. For the seek of completeness, we rewrite those solutions hereafter in a slightly different way, more convenient for our purpose. They can be written under the general expression

$$u(x,t) = 4\arctan[X(x)T(t)], \tag{21}$$

with the following *adaptation* to the boundary amplitude

$$X(L) = \tan(b/4), \tag{22}$$

tuning to the free-end condition

$$X_x(L) = 0, \tag{23}$$

and *synchronization* to the boundary period

$$T\left(t + \frac{2\pi}{\Omega}\right) = T(t). \tag{24}$$

The maximum amplitude of the periodic function $T(t)$ has been scaled to unity so as to let $X(x)$ to carry the information about the actual amplitude.

We define then the *output* $X(L) = A$, which actually serves as the basic variable of the problem, and write the following 3 solutions (for the seek of simplicity we do not assign an index to each solution and parameters but rather indicate to which case they correspond by a number in front of each equation):

$$\begin{aligned}
&(1)\ : X = A\ \mathrm{cn}[\mathrm{k(x-L)},\mu], && C_1 < A,\\
&(2)\ : X = A\ \mathrm{dn}[\mathrm{k(x-L)},\mu], && C_0 < A < C_1,\\
&(3)\ : X = \frac{A}{\mathrm{dn}[\mathrm{k(x-L)},\mu]}, && A < C_0,
\end{aligned} \tag{25}$$

with the reference amplitudes C_0 and C_1 given by

$$C_1^2 = \frac{1}{\Omega^2} - 1, \quad (1 + C_0^2)\mathbb{K}(C_0^2) = \frac{\pi}{2\Omega}, \tag{26}$$

where $\mathbb{K}$ denote the complete elliptic integral of the first kind. Note that the tuning (23) to the free end is automatically satisfied by the above 3 expressions. It is then straightforward to obtain the relation between the input, say $B = \tan(b/4)$, and the output A by evaluating the above expressions in $x = 0$

$$\begin{aligned}
&(1)\ : B = A\ \mathrm{cn}[\mathrm{kL},\mu],\\
&(2)\ : B = A\ \mathrm{dn}[\mathrm{kL},\mu],\\
&(3)\ : B = \frac{A}{\mathrm{dn}[\mathrm{kL},\mu]}.
\end{aligned} \tag{27}$$

where the A's vary in their allowed ranges. The bistable nature of the solution takes precisely its origin in the existence of the above three output amplitudes A corresponding to a single input B. The problem now is to express the parameters k and μ in terms of A.

In those three cases, the time part has the common structure

$$T = \mathrm{cn}(\omega(\mathrm{t} - \mathrm{t}_0), \nu), \tag{28}$$

where the initial phases are not relevant. In each case we have the following relations between the two new parameters ω (pseudo-frequency) and ν (argument):

$$\begin{aligned}
&(1)\ : \omega^2 = \frac{A^2}{1+A^2} \times \frac{1}{A^2 - (1+A^2)\nu^2},\\
&(2)\ : \omega^2 = \frac{A^2}{1+A^2} \times \frac{1}{A^2 + \nu^2},\\
&(3)\ : \omega^2 = \frac{A^2}{1+A^2} \times \frac{1}{A^2 + \nu^2}.
\end{aligned} \tag{29}$$

The synchronization requirement (24) now provides the relation allowing to compute ν from A by solving, in each of the 3 cases,

$$\Omega\mathbb{K}(\nu) = \frac{\pi}{2}\omega. \tag{30}$$

This equation does not furnish the explicit function $\nu(A)$, it is solved numerically in the 3 ranges $A > C_1$ for the solution (1), $A \in [C_0, C_1]$ for the solution (2) and $A \in [0, C_0]$ for the solution (3).

Once the equation (30) solved, the pseudo-wavenumbers k of the Jacobi elliptic functions in (25) obey

$$\begin{aligned}
&(1)\ : k^2 = \omega^2 - \frac{1-A^2}{1+A^2},\\
&(2)\ : k^2 = \omega^2 A^2,\\
&(3)\ : k^2 = \frac{1}{1+A^2} - \omega^2,
\end{aligned} \tag{31}$$

while the arguments are then explicitly given by

$$(1)\ : \mu^2 = \frac{1+A^2}{A^2} \times \frac{k^2}{1+k^2(1+A^2)},$$
$$(2)\ : \mu^2 = \frac{1+A^2}{A^2} - \frac{1}{k^2(1+A^2)}, \qquad (32)$$
$$(3)\ : \mu^2 = 1 + A^2 - \frac{A^2}{k^2(1+A^2)}.$$

Thus, from what precedes, every basic parameter ω, k, μ and ν is explicitly given in terms of the fundamental *"variable"* A.

In summary, the procedure to obtain the exact stationary solution to the boundary value problem (18), works as follows: solve the system (30) to get ν as a function of the output amplitude A (the variable) by replacing ω successively by its 3 expressions (29), compute then the arguments μ and wavenumbers k in terms of A only through (32) and (31), last the equations (27) furnish the sought relations between the input B and the output A. This is what we did in the case $L = 4$ and $\Omega = 0.5$ to obtain the continuous curves of Figure 4.

The determination of the threshold value b_s of the input amplitude $4 \arctan B$ is obtained then as follows. The function $B(A)$ defined by the equation (3) of (27) has an extremum at $A = A_0$ defined by

$$\frac{\partial}{\partial A}\left\{\frac{A}{\mathrm{dn}[\mathrm{kL}, \mu]}\right\}_{A=A_0} = 0, \qquad (33)$$

where both parameters k and μ are functions of A obtained through the procedure described here-above. Then we simply have $b_s = 4 \arctan[B(A_0)]$. Needless to say the expression of A_0 is not explicit and the procedure actually works numerically. In the chosen example ($L = 4$, $\Omega = 0.5$) we obtain by that method the threshold $b_s = 4.1$ while the approximate formula $4 \arctan \sqrt{1/\Omega^2 - 1}$ derived in the limit $L \to \infty$ gives $b_s = 4.19$.

References

1. H.M. Gibbs, S.L. McCall, T.N.C. Venkatesan, Phys. Rev. Lett. **36**, 1135 (1976)
2. H.G. Winful, J.H. Marburger, E. Garmire, Appl. Phys. Lett. **35**, 379 (1979)
3. W. Chen, D.L. Mills, Phys. Rev. B. **35**, 524 (1987)
4. N.D. Sankey, D.F. Prelewitz, T.G. Brown, Appl. Phys. Lett. **60**, 1427 (1992)
5. H.G. Winful, R. Zamir, S. Feldman, Appl. Phys. Lett. **58**, 1001 (1991)
6. O.H. Olsen, M.R. Samuelsen, Phys. Rev. B. **34**, 3510 (1986)
7. D. Barday, M. Remoissenet, Phys. Rev. B. **41**, 10387 (1990)
8. Y.S. Kivshar, O.H. Olsenand, M.R. Samuelsen, Phys. Lett. A **168**, 391 (1992)
9. F. Geniet, J. Léon, Phys. Rev. Lett. **89**, 134102 (2002)
10. J. Léon, Phys. Lett. A **319**, 130 (2003)
11. R. Khomeriki, Phys. Rev. Lett. **92**, 063905 (2004)
12. J. Léon, Phys. Rev. E **70**, 056604 (2004)
13. F. Geniet, J. Léon, J. Phys.: Condens. Matter **15**, 2933 (2003)
14. R. Khomeriki, J. Léon, Phys. Rev. E. **71**, 056620 (2005)
15. R. Khomeriki, J. Léon, Phys. Rev. Lett. **94**, 243902 (2005)
16. Chapters IV (by S.M. Girvin, A.H. MacDonald) and III (by J.P. Eisenstein) in *Perspectives in Quantum Hall Effect* edited by S. Das Sarma, A. Pinczuk (Wiley, New York, 1997)
17. X.G. Wen, A. Zee, Phys. Rev. B **47**, 2265 (1993)
18. Z.F. Ezawa, A. Iwazaki, Phys. Rev. B **48**, 15 189 (1993)
19. K. Yang, K. Moon, L. Belkhir, H. Mori, S.M. Girvin, A.M. MacDonald, L. Zheng, D. Yoshioka, Phys. Rev. B **54**, 11 644 (1996)
20. Y.E. Lozovik, A.V. Poushnov, Phys Lett. A **228**, 399 (1997)
21. M.M. Fogler, F. Wilczek, Phys. Rev. Lett. **86**, 1833 (2001)
22. H.J. Mikeska, J. Phys. C: Solid State Phys. **11**, L29 (1978)
23. G. Wysin, A.R. Bishop, P. Kumar, J. Phys. C: Solid State Phys. **17**, 5975 (1984)
24. I.B. Spielman, J.P. Eisenstein, L.N. Pfeiffer, K.W. West, Phys. Rev. Lett. **84**, 5808 (2000)
25. C.B. Hanna, A.H. MacDonald, S.M. Girvin, Phys. Rev. B **63**, 125305 (2001)
26. M. Remoissenet, *Waves Called Solitons* (Springer, Berlin, 1999)
27. A.C. Scott, *Nonlinear Science*, 2nd edn. (Oxford University Press, New York, 2003)
28. O.M. Braun, Yu.S. Kivshar, *The Frenkel-Kontorova Model: Concepts, Methods, and Applications* (Springer-Verlag, Berlin, 2004)
29. A film of the bifurcation of the pendula chain from low to large output amplitudes is presented on the web-page: `http://www.lpta.univ-montp2.fr/users/leon/Bistable/`
30. D. Barday, M. Remoissenet, Phys. Rev. B **41**, 10387 (1990)
31. H.S.J. van der Zant, M. Barahona, A.E. Duwel, T.P. Orlando, S. Watanabe, S. Strogatz, Physica D **119**, 219 (1998)
32. D. Chevriaux, R. Khomeriki, J. Léon, *Josephson superlattice at the onset of supratransmission*, in preparation